Identification of Membrane Topography of the Electrogenic Sodium Bicarbonate Cotransporter pNBC1 by in Vitro Transcription/Translation†

Sergei Tatishchev,‡ Natalia Abuladze,‡ Alexander Pushkin,‡ Debra Newman,‡ Weixin Liu,‡ David Weeks,§ George Sachs,§ and Ira Kurtz*,‡

Division of Nephrology, David Geffen School of Medicine at UCLA, Los Angeles, California 90095, and UCLA/Wadsworth Veteran Administration Hospital, Los Angeles, California 90073

Received September 9, 2002; Revised Manuscript Received November 18, 2002

ABSTRACT: The transmembrane topography of the human pancreatic electrogenic sodium bicarbonate cotransporter pNBC1 was investigated using in vitro transcription/translation of HK-M0 and HK-M1 fusion vectors designed to test membrane insertion properties of pNBC1 hydrophobic sequences (H). These vectors encode N-terminal 101 (HK-M0) or 139 (HK-M1) amino acids of the H,K-ATPase α-subunit, a linker region and the C-terminal 177 amino acids of the H,K-ATPase β-subunit that contain five N-linked glycosylation consensus sites (Bamberg, K., and Sachs, G. (1994) *J. Biol. Chem. 269*, 16909−16919). The glycosylation status of the β-region was used as a reporter to determine whether a given hydrophobic sequence possesses signal anchor and/or stop transfer properties in the HK-M0 and HK-M1 vectors. The linker region of each vector was replaced either with individual hydrophobic sequences or combinations thereof. The transcription/translation products of these fusion vectors in reticulocyte lysate system ± microsomal membranes were identified by [^{35}S]-autoradiography following separation using SDS−PAGE. The results of the in vitro transcription/translation analysis indicated that 10 (H1, H2N, H3, H5, H6, H7, H8, H9, H11, and H12) out of 12 hydrophobic sequences were able to insert into the plasma membrane. Two hydrophobic sequences, H4 and H10, had no membrane insertion activity even when upstream and downstream sequences were present. These data and immunocytochemical studies indicate that pNBC1 contains 10 transmembrane domains with N- and C-termini oriented intracellularly. This is the first characterization of the membrane topography of a sodium bicarbonate cotransporter.

The human pancreatic sodium bicarbonate cotransporter pNBC1[1] is an integral membrane protein expressed in pancreatic ducts, where it plays an important role in mediating basolateral bicarbonate influx necessary for transepithelial bicarbonate secretion (*1*−*3*). pNBC1 belongs to the family of the sodium bicarbonate cotransporters (NBCs) that mediate electrogenic and electroneutral sodium-bicarbonate cotransport. NBCs are members of the HCO_3^- transporter superfamily (BTS), which includes the Cl^-/HCO_3^- exchanger proteins AE1−AE3 (*4*, *5*), the Na^+-driven Cl^-/HCO_3^- exchangers (*6*−*8*), the electroneutral $Na^+-HCO_3^-$ cotransporter NBC3 (*9*, *10*) [splice variant NBC2 (*11*), rat orthologue NBCn1 (*12*)], and electrogenic $Na^+-HCO_3^-$ cotransporter isoform NBC4 (*13*−*15*).

The electrogenic sodium bicarbonate cotransporter pNBC1 is encoded in humans by the SLC4A4 gene (*16*), which also encodes the proximal tubule electrogenic sodium bicarbonate cotransporter kNBC1 (*7*, *17*−*19*). pNBC1 and kNBC1 are 93% identical, but with 85 N-terminal amino acids of pNBC1 replaced by 41 distinct amino acids in kNBC1. pNBC1, besides being expressed in the pancreas, is also expressed at a lower level in several other organs including duodenum, colon, heart, salivary gland, eye, brain, prostate, testis, and thyroid (*3*, *20*, *21*), whereas kNBC1 is expressed in kidney and eye (*17*−*22*). Depending on the specific cell type, these cotransporters are thought to play an important role in mediation of transepithelial sodium and bicarbonate transport, regulation of intracellular pH, as well as maintenance of extracellular pH.

Although electrogenic and electroneutral sodium bicarbonate cotransport proteins have been recently functionally characterized, relating their transport properties to a mechanistic transport model requires improved understanding of their topographic organization. To date, the anion exchanger AE1 is the only member of the BTS, which has been extensively structurally characterized (*23*−*30*) Previous studies have clearly defined the first eight transmembrane segments, however the topography of the carboxy-terminal region remains controversial (*23*, *29*, *30*). Using a cysteine-directed approach, Fujinaga et al. proposed a model for the anion exchanger AE1, wherein the transporter contains 13 α-helical transmembrane segments (*28*).

† This work was supported by NIH Grants DK-58563 and DK-07789, the Max Factor Family Foundation, the Richard and Hinda Rosenthal Foundation, and the NKF of Southern California J891002 to I.K..

* Corresponding author. Address: Room 7-155 Factor Bldg., 10833 Le Conte Ave., Los Angeles, CA 90095. E-mail: Ikurtz@mednet.ucla.edu. Tel: 310-2066741. Fax: 310-8256309.

‡ David Geffen School of Medicine at UCLA.

§ UCLA/Wadsworth Veteran Administration Hospital.

[1] Abbreviations: pNBC1, sodium bicarbonate cotransporter 1 (pancreatic variant); kNBC1, sodium bicarbonate cotransporter 1 (kidney variant); SA, signal anchor sequence; ST, stop transfer sequence; CCK-A, cholecystokinin-A; NHE3, Na^+/H^+ exchanger 3.

10.1021/bi026826q CCC: $25.00
Published on Web 12/28/2002

Table 1: Putative Hydrophobic Sequences of pNBC1 in HK-M0 and HK-M1 Vectors and Summary of Transcription/Translation Results[a]

insert	sequence	position	glycosylation in HK-M0	glycosylation in HK-M1	activity
H1	−ALSAILFIYLATVTNAITFG−	469−488	+	−	SA/ST
H2C	−AVSGAIFCLFAGQPLTILSSTGPVLVF−	509−535	−	+	−/−
H2N	−FLGTAVSGAIFCLFAGQPLTIL−	505−526	+	−	SA/ST
H3	−LWIGLWSAFLCLILVATDASFLV−	555−577	+	+	SA/ST
H3CE	−LWIGLWSAFLCLILVATDASFLVQYF−	555−580	+	−	SA/ST
H4	−FTEEGFSSLISFIFIYDAF−	583−601	−	+	−/−
H4CE	−FTEEGFSSLISFIFIYDAFKKMIKLA −	583−608	−	+	−/−
H4CS	−SLISFIFIYDAFKKMIKLA −	590−608	−	+	−/−
H5	−ITLMSFILFLGTYTSSMAL−	692−710	+	−	SA/ST
H6	−LISDFAIILSILIFCVIDALVGV−	726−748	+	+	SA/ST
H7	−WWVCLAAAIPALLVTILIFM−	778−797	+	−	SA/ST
H8	−LFWVAILMVICSLMALPWYVAA−	823−844	+	+	SA/ST
H8CE	−LFWVAILMVICSLMALPWYVAATVI−	823−847	+	+	SA/ST
H9	−LVFILTGLSVFMAPILKFI−	882−900	+	+	SA/ST
H9CE	−LVFILTGLSVFMAPILKFIPMP−	882−903	+	−	SA/ST
H10	−VLYGVFLYMGVASLNGVQFM−	904−923	−	+	−/−
H11	−VHLFTFLQVLCLALLWIL−	950−967	+	−	SA/ST
H12	−VAAIIFPVMILALVAV−	971−986	+	−	SA/ST
H3−H4	−LWIGL...IYDAF−	555−601	+	−	
H2N−H4	−FLGTA...IYDAF−	505−601	−	+	
H9−H11	−LVFIL...LLWIL−	882−967	+	+	

[a] Presented are the designations, the amino acid sequences of the putative hydrophobic pNBC1 inserts tested, their positions, the presence or absence of glycosylation in the HK-M0/M1 vectors, and their signal anchor (SA)/stop transfer (ST) activity. + stands for the presence of glycosylation, and − stands for the absence of glycosylation. Where the sequences were too long to list, the N- and C-termini of the sequences are listed connected by dots.

A description of the topography of sodium bicarbonate cotransporters will help elucidate the structural motifs responsible for ion binding and permeation. A variety of algorithms predict the presence of 9−11 hydrophobic transmembrane domains. In the current study, we have utilized an in vitro transcription/translation technique coupled with results of immunostaining to determine the membrane topography of human pNBC1. This methodology has been successfully used to determine membrane topography of several membrane transport proteins, such as the gastric H,K-ATPase (*31*), the ER−Ca-ATPase (*32*), the cadA P-type ATPase from *H. pylori* (*33*), the rabbit gastric CCK-A receptor (*34*), the intestinal Na-bile acid cotransporter (*35*), and Na^+/H^+ exchanger NHE3 (*36*). In vitro transcription/translation analysis of the cadA P-type ATPase and the CCK-A receptor provided unambiguous definition of the transmembrane segments of these polytopic integral membrane proteins, whereas analysis of the bile acid cotransporter and NHE3 resulted in two possible membrane insertion models but excluded other hypotheses. Using this method here, an unambiguous topographic model for pNBC1 was generated.

EXPERIMENTAL PROCEDURES

Construction of HK-M0 and HK-M1 Vectors. The coding region of human pNBC1 was cloned into the *Eco*RI and *Eco*RV sites in the pcDNA3.1 vector (Clontech, Palo Alto, CA). Two expression plasmids, HK-M0 and HK-M1, were used to analyze the topogenic properties of putative transmembrane segments of pNBC1. HK-M0 and HK-M1 vectors were constructed in the pGEM7zf+ (ΔHindIII) plasmid as previously described in detail (*31*).

HK-M0 Vector. The HK-M0 vector enables analysis of signal anchor (SA) sequences. The vector begins with 314 nucleotides (−12 to 302) coding for the first 101 amino acids of the α-subunit of the rabbit gastric H,K-ATPase. The α-subunit contains a putative cytoplasmic anchor sequence consisting of eight positively charged amino acids between positions 25 and 39. The end of the vector encodes the reporter sequence containing the C-terminal 177 amino acids of the H,K-ATPase *β*-subunit. This sequence contains five of the original consensus sequences for the *N*-linked glycosylation of the *β*-subunit and lacks any transmembrane activity. To allow insertion of variable sequences between the derivatives of the α- and *β*-subunits, the vector contains a linker sequence that has two restriction sites, *Bgl*II and *Hind*III (*37*).

HK-M1 Vector. The HK-M1 vector enables analysis of stop transfer (ST) sequences. This vector is identical to the HK-M0 vector, except for the N-terminal region. The HK-M1 vector contains 425 nucleotides (−12 to 413) coding for the first 139 amino acids of the rabbit gastric H,K-ATPase α-subunit, which constitute the first transmembrane segment of the H,K-ATPase (*37*).

Variable Segment. The sequences coding for putative transmembrane segments of pNBC1 (Table 1) were synthesized by PCR such that sense primers contained the *Bgl*II site and antisense primers contained the *Hind*III site. The sequences then were ligated into the corresponding *Bgl*II and *Hind*III sites of the HK-M0 and HK-M1 vectors. The primer sequences and conditions for the amplification were determined using OLIGO 4.0 primer analysis software (National Biosciences, Plymouth, MN).

The difference between HK-M0 and HK-M1 vectors allows determination of the topographic properties of putative transmembrane segments using in vitro transcription/translation in the presence of canine pancreatic microsomal membranes. The native HK-M0 vector does not contain a transmembrane segment and therefore is not glycosylated in the presence of microsomes. The native HK-M1 vector, on the other hand, contains the first transmembrane segment of the H,K-ATPase allowing the entry of the *β*-subunit

reporter sequence into the lumen of the microsomes and its subsequent glycosylation, which is revealed by a ~12.5 kDa mobility shift on SDS−PAGE. If a sequence encoding a transmembrane segment is present in the linker region of the HK-M0 vector, the β-subunit reporter is transported into the lumen of the microsomes, resulting in glycosylation of the fusion protein, whereas a transmembrane segment introduced into the HK-M1 vector translocates the reporter sequence out of the lumen of the microsomes, thus preventing glycosylation. Any variable sequence that causes glycosylation of the C-terminus of HK-M0 is characterized as an SA sequence, while any variable sequence that prevents glycosylation of the C-terminus of HK-M1 is characterized as an ST sequence (*31*−*33*). Integral membrane proteins usually fold co-translationally as alternating SA and ST sequences, but occasionally membrane insertion is posttranslational, depending on insertion of other parts of the protein or even of another membrane inserted protein as in the case of the Na,K and H,K-ATPases (*31*, *32*).

Vector Amplification and Purification. The expression vectors containing variable sequences coding for different fusion proteins were replicated in *E. coli* DH5α (Invitrogen, Carlsbad, CA) and isolated using anion-exchange columns (Qiagen, Chatsworth, CA). The cDNA inserts were first screened by restriction analysis of DNA minipreps and then by PCR with subsequent dideoxy sequencing. The PCR products were obtained using a sense primer complementary to a sequence ~90 nucleotides upstream from the *Bgl*II site. All cDNA inserts were verified by sequence analysis using GeneWorks Software 2.0 (Oxford, England)

PCR and Cloning. A typical 50 μL reaction mixture contained 1 ng of the DNA template, 0.25 μM concentration of each primer, 200 μM dNTPs (Pharmacia-Amersham, Piscataway, NJ), the buffer provided by the manufacturer, and 1 unit of Taq polymerase (Takara Biomedicals, Kyoto, Japan). The Expand Long Template PCR System (Roche, Mannheim, Germany) was used for the longer DNA fragments in accordance with the manufacturer's protocol. The PCR products coding for the individual variable segments and their pairs were digested with *Bgl*II and *Hind*III enzymes and inserted into the corresponding vectors (*38*).

In Vitro Transcription/Translation. To determine the membrane insertion properties of all the selected sequences, the fusion proteins encoded by the HK-M0 or HK-M1 vectors were expressed using the TNT Quick Coupled Transcription/Translation System (Promega, Madison, WI) in the presence of [^{35}S]-methionine (Pharmacia-Amersham) and canine pancreatic microsomal membranes (Promega) according to the manufacturer's protocol. Reaction mixtures without the microsomal membranes provided the negative control. In each transcription/translation experiment, the native HK-M0 and HK-M1 vectors were used to control the efficiency of the reaction and to verify glycosylation activity of the microsomes used. Each transcription/translation reaction was performed at least three times.

SDS−PAGE and Autoradiography. The translation products were separated on 10−20% Tris-Tricine gels (Bio-Rad, Hercules, CA) that were subsequently fixed in 45% methanol/10% acetic acid for 45 min, washed in distilled water for 5 min, and then dried. The products synthesized in the absence or presence of the microsomal membranes using the same vector were run in lanes next to each other. Molecular mass standards were obtained from Bio-Rad. Dry gels were placed into a cassette containing Kodak BioMax film (Rochester, NY) and were exposed for 14−16 h at room temperature. The presence of glycosylation was seen by the increase in molecular weight (~12.5 kDa) of the translated product in the presence of microsomes as compared to the translation without microsomal membranes.

Deglycosylation. After the transcription/translation reaction, the microsomal membranes were solubilized in denaturation buffer and treated with endoglycosidase H (Roche) according to the manufacturer's protocol. The products of the reaction were separated using SDS−PAGE, and radioactivity was determined using Kodak film as described above. This procedure confirmed that glycosylation was responsible for the 12.5 kDa molecular weight shift on the autoradiograms.

Immunocytochemistry. The predicted intracellular localization of the N- and C-termini of pNBC1 was defined by using an immunocytochemical approach (*39*). HEK-293T cells grown on fibronectin coated cover slips were transfected using the calcium phosphate precipitation method (transfection efficiency (80%) with either a plasmid (pcDNA3.1, Invitrogen) containing the coding region for pNBC1 or mock-transfected with the pcDNA3.1 plasmid only. The cells were either rinsed in PBS alone, or in methanol for permeabilization of the plasma membrane at −20 °C for 5 min and then washed in PBS several times. The pNBC1 specific polyclonal N-terminal antibody used in this study has been previously characterized (*21*). The pNBC1 polyclonal C-terminal antibody used in this study was raised against amino acids 1045−1050. The labeling with each antibody was blocked when incubated with their respective immunizing peptides. Each primary antibody (1:100 dilution) was applied for 1 h and following several washes in PBS, goat anti-rabbit IgG conjugated with Alexa 594 (1/500 dilution, Molecular Probes) was applied for an additional 1 h. The slides were washed in PBS and mounted in Cytoseal 60 (Stephens Scientific, Riverdale, NJ). Confocal images were captured with a Leica TCS SP inverted confocal Microscope (Leica, Germany) using a krypton laser (model 643, Melles Griot, Irvine, CA). The experiments were performed in duplicate, and a minimum of 500 transfected cells was analyzed in each protocol.

Materials. All chemicals used were analytical grade or higher. Molecular biological reagents were obtained from Promega, Qiagen, Bio-Rad, Amersham, Takara, Invitrogen, and Roche as specified.

RESULTS

Hydropathy Analysis. Various hydropathy algorithms were used as a guide for the prediction of the number and the boundaries of all hydrophobic sequences that constitute putative transmembrane domains (TM) of pNBC1 (Table 2). On the basis of these computer-generated models, we constructed various fusion vectors and tested their SA/ST properties. The amino acid sequences that inserted into the microsomal membranes are designated by shaded regions, and 10 of these correspond to regions of hydrophobicity shown in the Kyte−Doolittle hydropathy plot for the human pNBC1 in Figure 1. Two hydrophobic regions that did not insert into the membranes are underlined (Figure 1). Hence,

Table 2: Hydropathy Predictions of Putative Transmembrane Domains (PTM) of the Human pNBC1

PTM	Kyte−Doolittle (*47*)	GES scale (*55*)	Persson & Argos (*56*)	MEMSAT (*57*)	SOSUI (*58*)	TMpred (*48*)	TMHMM (*59*)	HMMTOP (*60*)
1	467−487	470−490	462−490	469−491	469−491	469−488	469−491	456−480
2	500−520	504−524	500−526	512−535	509−531	505−526	504−526	511−535
3	553−573	553−573	556−576	555−577	559−581	555−577	555−577	556−580
4	586−606		582−602			583−601	590−608	
5	686−706	690−710	687−709	692−710	697−719	692−710	692−710	692−710
6	729−749	726−746	723−751	726−748	727−749	727−748	730−748	731−748
7	778−798	777−797	775−803	778−797	778−800	779−797	778−796	779−796
8	821−841	823−843	821−849	823−847	826−848	823−844	816−838	823−847
9	878−898	878−898	883−911	878−897	888−910	882−906	879−897	878−897
10				904−920		899−923	904−922	904−923
11			954−982		942−964	950−976		954−978
12	968−988	966−986		962−986	966−986		962−984	

Listed are the putative transmembrane domains of pNBC1 that were predicted by eight different computer algorithms used to analyze the membrane topography of pNBC1. The computer-predicted transmembrane domains were used for selecting the putative hydrophobic sequences for the transcription/translation studies.

a model of the topography of pNBC1, which is supported by the results from the data presented here, is shown in Figure 2. This method does not define the exact boundaries of the transmembrane segments and perhaps charged or hydrophilic amino acids close to the either end of the segments defines their boundaries.

HK-M0 and HK-M1 Fusion Proteins. The native HK-M0 vector does not contain an amino acid sequence that possesses transmembrane properties. As a result, the β-region of the HK-M0 fusion protein is not translocated into the lumen of the microsomes and therefore is not glycosylated (*31*). As shown in Figure 3, lanes 1 and 2, the in vitro transcription/translation product of the native HK-M0 vector showed no shift in molecular weight in the presence of microsomal membranes. In contrast, the HK-M1 vector product showed a 12.5 kDa shift in molecular weight in the presence of microsomal membranes (Figure 3, lanes 3 and 4). The shift occurs due to glycosylation of the five glycosylation consensus sequences present within the β-region. The glycosylation shift observed in the presence of microsomal membranes was removed by the treatment with endoglycosidase H (data not shown). This indicates that the product of the HK-M1 vector contains a hydrophobic sequence (α-subunit M1) capable of acting as an SA sequence and therefore translocating the reporter β-region into the lumen of the microsomes (*31*).

HK-M0 and HK-M1Vector Analysis of pNBC1 Putative Hydrophobic Sequences. To analyze the topographic properties of putative transmembrane domains of pNBC1 predicted by the hydropathy analyses shown in Table 2, selected hydrophobic sequences, individually or in combination, were introduced into the HK-M0 and HK-M1 vectors. The presence or absence of glycosylation allowed analysis of whether the selected sequences are capable of inserting into the membrane. All glycosylated products were treated with endoglycosidase to confirm that a 12.5 kDa shift in molecular weight is due to glycosylation (data not shown).

H1. The hydrophobic sequence H1 (amino acids 469−488, Figure 1) inserted in the HK-M0 vector promoted the glycosylation of the reporter β-region in the presence of microsomal membranes (Figure 4, lanes 1 and 2). The observed 12.5 kDa glycosylation shift indicated that H1 acts as an SA sequence, in agreement with its position as the first transmembrane sequence. The same cDNA sequence inserted into the HK-M1 vector prevented the glycosylation of the β-region in the presence of microsomes, indicating that H1 also acts as an ST sequence (Figure 4, lanes 3 and 4). According to the proposed pNBC1 topography model (Figure 2), this H1 sequence corresponds to putative TM1.

H2. Two different hydrophobic sequences, H2C and H2N (Table 1) between amino acids 505 and 535, were inserted into the HK-M0 and HK-M1 vectors. The H2C insert (amino acids 509−535) did not promote the glycosylation of the β-region in the HK-M0 vector (Figure 4, lanes 5 and 6) and did not prevent the glycosylation of the same reporter region in the HK-M1 vector (Figure 4, lanes 7 and 8). The H2C insert thus exhibited neither SA nor ST properties. On the other hand, the H2N insert (amino acids 505−526, Figure 1) acted as both an SA and an ST sequence. H2N in the HK-M0 vector caused a 12.5-kDa shift in molecular weight of the translated protein in the presence of microsomal membranes (Figure 4, lanes 9 and 10). Furthermore, H2N in the HK-M1 vector prevented the glycosylation of the β-region in the presence of microsomal membranes (Figure 4, lanes 11 and 12). In the proposed pNBC1 topography model (Figure 2), H2N corresponds to putative TM2 which is predicted to have an ST orientation in the context of the natural sequence.

H3. Insertion of the hydrophobic sequence H3 (amino acids 555−577) into the HK-M0 vector resulted in glycosylation of the translated fusion protein in the presence of microsomal membranes (Figure 4, lanes 13 and 14), indicating that H3 acts as an SA sequence. The same sequence present in the HK-M1 vector reduced but did not completely prevent the glycosylation of the fusion protein (Figure 4, lane 15 and 16). The band corresponding to the 12.5 kDa glycosylation shift in lane 16 (Figure 4) was removed by the treatment with endoglycosidase. When the H3 was C-terminally elongated, the new insert H3CE (amino acids 555−580, Figure 1) promoted not only strong glycosylation of the β-region in the HK-M0 vector (Figure 4, lane 17 and 18), but also completely prevented glycosylation in the HK-M1 vector in the presence of microsomal membranes (Figure 4, lane 19 and 20). The H3CE insert corresponds to an SA-acting putative TM3 in our proposed pNBC1 topography model (Figure 2).

H4. Translation of the hydrophobic sequence H4 (amino acids 583−601, Figure 1, underlined), inserted into the HK-

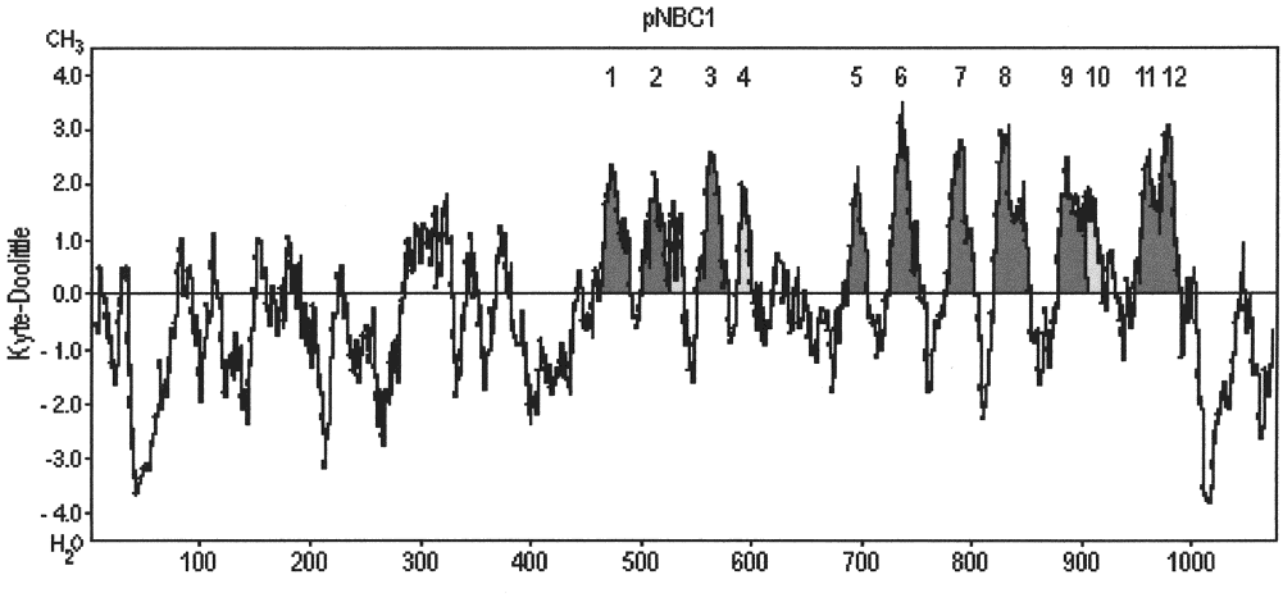


```
MEDEAVLDRG ASFLKHVCDE EEVEGHHTIY IGVHVPKSYR RRRRHKRKTG HKEKKEKERI SENYSDKSDI ENADESSSSI   80
LKPLISPAAE RIRFILGEED DSPAPPQLFT ELDELLAVDG QEMEWKETAR WIKFEEKVEQ GGERWSKPHV ATLSLHSLFE  160
LRTCMEKGSI MLDREASSLP QLVEMIVDHQ IETGLLKPEL KDKVTYTLLR KHRHQTKKSN LRSLADIGKT VSSASRMFTN  240
PDNGSPAMTH RNLTSSSLND ISDKPEKDQL KNKFMKKLPR DAEASNVLVG EVDFLDTPFI AFVRLQQAVM LGALTEVPVP  320
TRFLFILLGP KGKAKSYHEI GRAIATLMSD EVFHDIAYKA KDRHDLIAGI DEFLDEVIVL PPGEWDPAIR IEPPKSLPSS  400
DKRKNMYSGG ENVQMNGDTP HDGGHGGGGH GDCEELQRTG RFCGGLIKDI KRKAPFFASD FYDALNIQAL SAILFIYLAT  480
VTNAITFGGL LGDATDNMQG VLESFLGTAV SGAIFCLFAG QPLTILSSTG PVLVFERLLF NFSKDNNFDY LEFRLWIGLW  560
SAFLCLILVA TDASFLVQYF TRFTEEGFSS LISFIFIYDA FKKMIKLADY YPINSNFKVG YNTLFSCTCV PPDPANISIS  640
NDTTLAPEYL PTMSSTDMYH NTTFDWAFLS KKECSKYGGN LVGNNCNFVP DITLMSFILF LGTYTSSMAL KKFKTSPYFP  720
TTARKLISDF AIILSILIFC VIDALVGVDT PKLIVPSEFK PTSPNRGWFV PPFGENPWWV CLAAAIPALL VTILIFMDQQ  800
ITAVIVNRKE HKLKKGAGYH LDLFWVAILM VICSLMALPW YVAATVISIA HIDSLKMETE TSAPGEQPKF LGVREQRVTG  880
TLVFILTGLS VFMAPILKFI PMPVLYGVFL YMGVASLNGV QFMDRLKLLL MPLKHQPDFI YLRHVPLRRV HLFTFLQVLC  960
LALLWILKST VAAIIFPVMI LALVAVRKGM DYLFSQHDLS FLDDVIPEKD KKKKEDEKKK KKKKGSLDSD NDDSDCPYSE 1040
KVPSIKIPMD IMEQQPFLSD SKPSDRERSP TFLERHTSC                                            1079
```

FIGURE 1: Kyte−Doolittle hydropathy profile of the human pNBC1 and its primary amino acid sequence. The hydropathy plot of pNBC1 was calculated by the method of Kyte−Doolittle using an 11 amino acid window. The numbers at the top indicate the 12 putative hydrophobic sequences of the cotransporter that were predicted by various computer algorithms (Table 2) and tested for membrane insertion properties using in vitro transcription/translation analysis. The corresponding peaks of the plot are shaded. The 1079 amino acids of pNBC1 are shown below the plot. Highlighted amino acids correspond to the membrane inserted sequences, while underlined regions correspond to relatively hydrophobic sequences that did not show any membrane insertion activity.

M0 vector, did not promote glycosylation of the β-region in the presence of microsomal membranes (Figure 5, lanes 1 and 2), and its insertion in the HK-M1 vector did not prevent glycosylation of the translated product (Figure 5, lanes 3 and 4). Even when the insert was extended at its C-terminus to amino acid 608 (Table 1; H4CE) or the sequence was C-terminally shifted to a position between amino acids 590 and 608 (Table 1; H4CS), the sequence displayed neither SA nor ST activity, lanes 1−4. Hence, H4 lacks an SA and ST activities when inserted alone into the HK-M0 and HK-M1 vectors.

H3−H4 Construct (amino acids 555−601). The construct composed of hydrophobic sequences H3 and H4 was used to determine whether the N-terminal amino acid sequence including H3 can provide the H4 sequence with an ST activity, as expected given that H4 follows the H3 signal anchor sequence. Insertion of the H3−H4 construct into the HK-M0 vector resulted in glycosylation of the translated product in the presence of microsomal membranes (Figure 5, lanes 5 and 6), as for H3CE alone, while insertion of the same sequence into the HK-M1 vector prevented glycosylation of the translated product in the presence of microsomes (Figure 5, lanes 7 and 8), again as H3CE alone. Since H3CE has been shown to possess an SA activity, these data indicate that the inserted sequence H3−H4 does not contain a pair of transmembrane domains and H4 does not have trans-

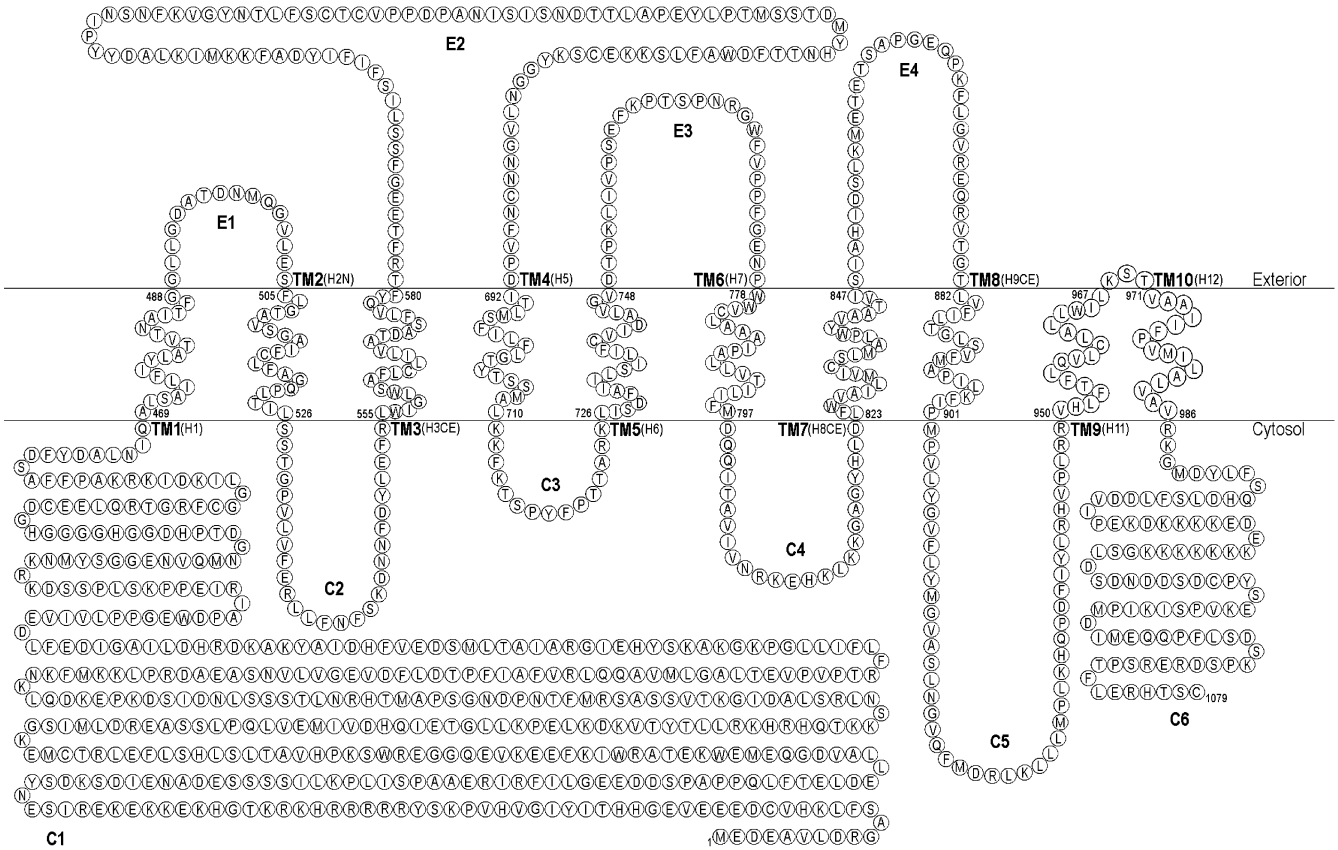

FIGURE 2: Primary amino acid sequence and predicted topological structure of the human pNBC1. Shown are the transmembrane domains in the proposed pNBC1 model which are based on the predictions deduced from computer algorithm analyses of the pNBC1 primary structure and results obtained by the in vitro transcription/translation technique and immunocytochemical studies. The transmembrane domains of pNBC1 are numbered (TM1−10) and presented with the corresponding hydrophobic sequences (H) that were shown to possess transmembrane activity. The amino acid residues in each TM as illustrated are in general determined by the presence of hydrophilic amino acids (TM2−10) likely to be at the membrane boundary or by a turn motif such as PMP in TM8. E stands for extracellular loop, and C stands for cytoplasmic loop.

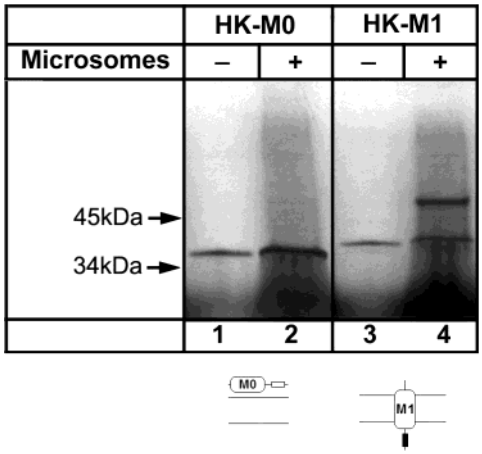

FIGURE 3: In vitro transcription/translation of the native HK-M0 and HK-M1 vectors without the inserts. SDS−PAGE analysis of the products obtained by in vitro transcription/translation of the HK-M0 vector (lanes 1 and 2) and HK-M1 vector (lanes 3 and 4), in the absence (−) and presence (+) of microsomal membranes. [^{35}S]Met-labeled products were visualized by autoradiography. An oval with "MO" represents the first 101 amino acids of the α-subunit of the rabbit gastric H,K-ATPase. An oval with "M1" represents the first 139 amino acids of the rabbit gastric H,K-ATPase α-subunit. A filled rectangle represents the glycosylated *β*-region, and an open rectangle represents the nonglycosylated *β*-region.

membrane activity even when in context with the preceding transmembrane domain. Thus, H4 does not act as a transmembrane sequence alone or in context with the upstream transmembrane sequence.

H2N−H4 Construct (amino acids 505−601). To confirm whether H4 is a part of pNBC1 transmembrane topography, we inserted the H2N−H4 construct into the HK-M0 and HK-M1 vectors. Incorporation of the H2N−H4 sequence into the HK-M0 vector did not cause the 12.5 kDa glycosylation shift in molecular weight of the translated protein in the presence of microsomal membranes (Figure 5, lanes 9 and 10). Insertion of the same sequence into HK-M1 vector promoted glycosylation of the translated product in the presence of microsomal membranes (Figure 5, lanes 11 and 12). These data indicate that the inserted sequence contains a single pair of transmembrane domains. Given that H2N and H3CE exhibited membrane insertion properties, the two transmembrane domains are represented by H2N and H3CE, making the H4 sequence a part of an extra-membranous loop, and not a part of the transmembrane domain.

H5. The presence of the H5 sequence (amino acids 692−710, Figure 1) in the HK-M0 vector resulted in glycosylation of the *β*-region of the fusion protein (Figure 5, lanes 13 and 14), indicating that H5 acts as an SA sequence. When the same sequence was inserted in the HK-M1 vector, the glycosylation of the fusion protein was completely prevented indicating that H5 acts as an ST sequence (Figure 5, lane 15 and 16). Since H4 lacks transmembrane activity, H5 takes its place as putative TM4, which is predicted to have an ST

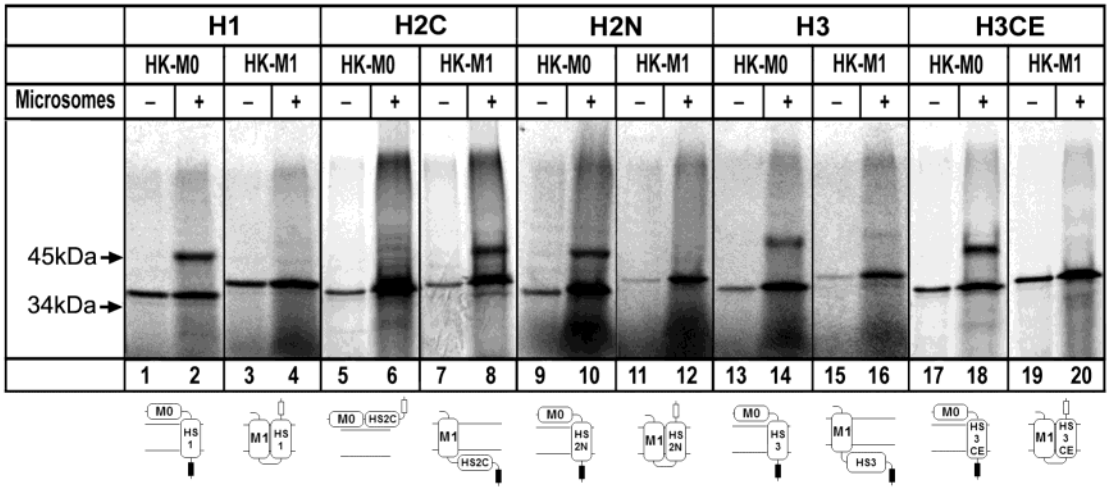

FIGURE 4: SDS−PAGE analysis of the [^{35}S]Met-labeled fusion proteins obtained by in vitro transcription/translation of the HK-M0 and HK-M1 vectors, in the absence (−) and presence (+) of microsomal membranes. The HK-M0 and HK-M1 vectors contain putative hydrophobic sequences H1 (lanes 1−4), H2C (lanes 5−8), H2N (lanes 9−12), H3 (lanes 13−16), and H3CE (lanes 17−20). A filled rectangle represents the glycosylated β-region, and an open rectangle represents the nonglycosylated β-region.

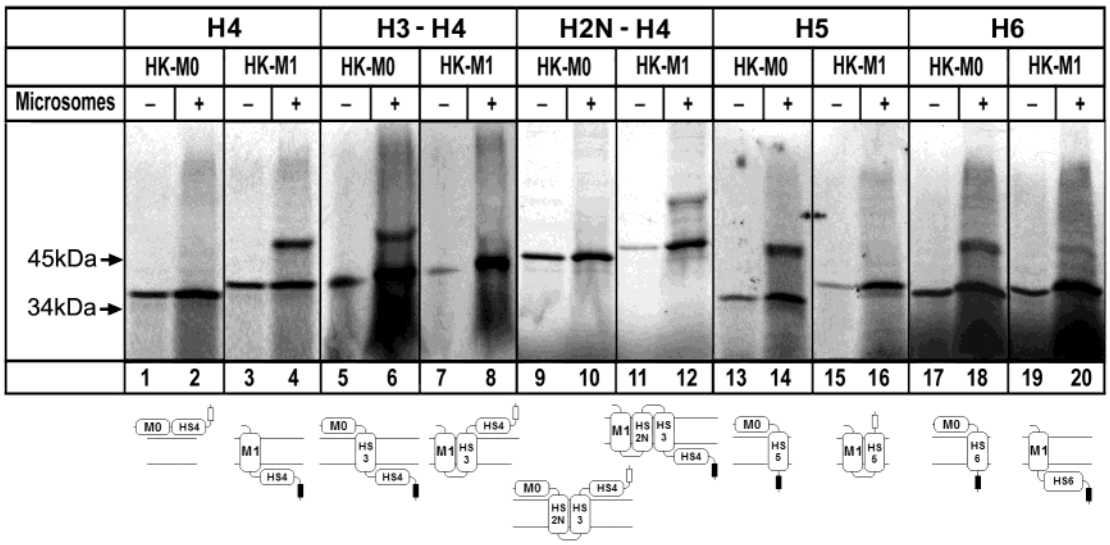

FIGURE 5: SDS−PAGE analysis of the [^{35}S]Met-labeled fusion proteins obtained by in vitro transcription/translation of the HK-M0 and HK-M1 vectors, in the absence (−) and presence (+) of microsomal membranes. The HK-M0 and HK-M1 vectors contain putative hydrophobic sequences H4 (lanes 1−4), H5 (lanes 13−16), H6 (lanes 17−20), and constructs H3−H4 (lanes 5−6) and H2−H4 (lanes 9−12). A filled rectangle represents the glycosylated β-region, and an open rectangle represents the nonglycosylated β-region.

orientation in the proposed pNBC1 topography model (Figure 2).

H6. Insertion of the hydrophobic sequence H6 (amino acids 727−748, Figure 1) into the HK-M0 vector resulted in the glycosylation of the translated fusion protein in the presence of microsomal membranes (Figure 5, lanes 17 and 18), which indicates that H6 acts as an SA sequence. When H6 sequence was inserted into the HK-M1 vector, it did not completely prevent the glycosylation of the β-region of the fusion protein (Figure 5, lane 19 and 20). The remaining weak glycosylation band in the lane 20 of the Figure 5 was removed following treatment with endoglycosidase. The glycosylation band of low intensity appearing in this case indicates that H6 corresponding to putative TM5 acts as a relatively weak ST sequence. TM5 is predicted to have an SA rather than an ST orientation in the proposed topography model of pNBC1 (Figure 2).

H7. The hydrophobic sequence H7 (amino acids 778−797, Figure 1) inserted into the HK-M0 vector resulted in a 12.5-kDa shift in molecular weight of the translated protein in the presence of microsomal membranes (Figure 6, lanes 1 and 2). Insertion of the same sequence into the HK-M1 vector prevented the glycosylation of the β-region in the presence of microsomal membranes (Figure 6, lanes 3 and 4). The H7 therefore acts as both SA and ST sequence. In the proposed pNBC1 topography model (Figure 2), H7 corresponds to putative TM6, which is predicted to have an ST orientation in the plasma membrane.

H8. Insertion of the H8 sequence (amino acids 823−844) into the HK-M0 vector promoted a weak glycosylation of the translated fusion protein in the presence of microsomal membranes (Figure 6, lanes 5 and 6). There was also a weak glycosylation when the H8 sequence was inserted into the HK-M1 vector (Figure 6, lanes 7 and 8). The low-intensity bands corresponding to the 12.5 kDa glycosylation shift in the lanes 6 and 8 of the Figure 6 disappeared with deglycosylation (data not shown). When the H8 sequence was C-terminally extended, this new insert H8CE (amino

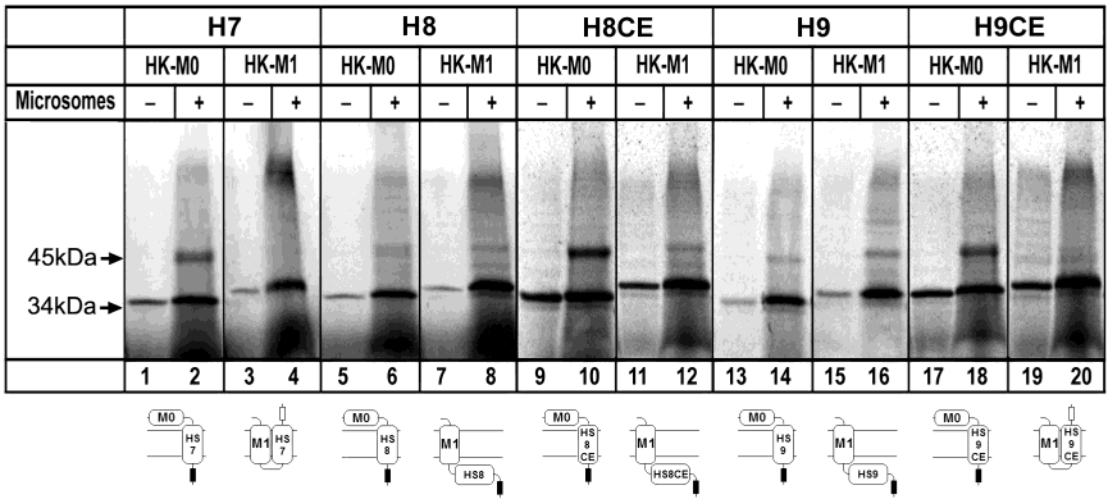

FIGURE 6: SDS−PAGE analysis of the [^{35}S]Met-labeled fusion proteins obtained by in vitro transcription/translation of the HK-M0 and HK-M1 vectors, in the absence (−) and presence (+) of microsomal membranes. The HK-M0 and HK-M1 vectors contain putative hydrophobic sequences H7 (lanes 1−4), H8 (lanes 5−8), H8CE (lanes 9−12), H9 (lanes 13−16), and H9CE (lanes 17−20). A filled rectangle represents the glycosylated β-region, and an open rectangle represents the nonglycosylated β-region.

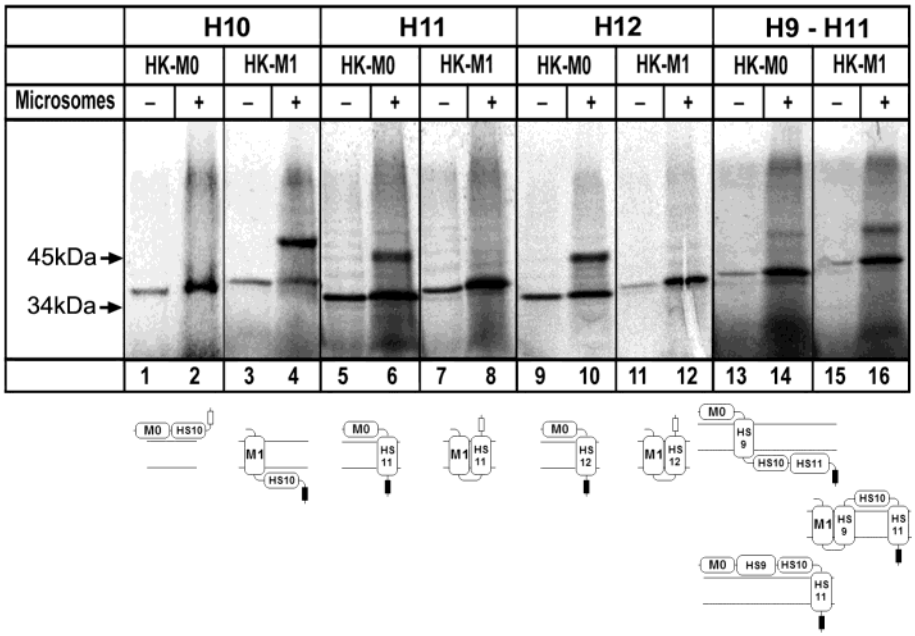

FIGURE 7: SDS−PAGE analysis of the [^{35}S]Met-labeled fusion proteins obtained by in vitro transcription/translation of the HK-M0 and HK-M1 vectors, in the absence (−) and presence (+) of microsomal membranes. The HK-M0 and HK-M1 vectors contain putative hydrophobic sequences H10 (lanes 1−4), H11 (lanes 5−8), H12 (lanes 9−12), and construct H9−H11 (lanes 13−16). A filled rectangle represents the glycosylated β-region, and an open rectangle represents the nonglycosylated β-region.

acids 823−847, Figure 1) promoted a strong glycosylation of the β-region of the fusion protein in the HK-M0 vector (Figure 6, lanes 9 and 10). However, insertion of the H8CE into the HK-M1 vector resulted, similarly to the H8 insert, in retention of a weak glycosylation signal (Figure 6, lanes 11 and 12). These data indicate that H8CE corresponding to putative TM7 acts as an SA and a weak ST sequence, as expected from its position in the proposed pNBC1 model (Figure 2).

H9. The presence of H9 (amino acids 882−900) in the HK-M0 and HK-M1 vectors resulted in a weak glycosylation of the translated fusion protein in the presence of microsomal membranes (Figure 6 lanes 13−16). The faint glycosylation bands in the lanes 14 and 16 of the Figure 6 disappeared upon treatment with endoglycosidase H (data not shown). Extension of the H9 insert at its C-terminus (amino acids 882−903, Figure 1) produced a hydrophobic sequence H9CE, which in the HK-M0 vector caused a strong glycosylation of the translated product (Figure 6, lanes 17 and 18). The H9CE sequence in the HK-M1 vector completely prevented glycosylation of the translated product (Figure 6, lanes 19−20). Thus, H9CE exhibits both SA and ST properties. In the proposed pNBC1 model (Figure 2), H9CE corresponds to putative TM8.

H10. Insertion of the sequence coding for H10 (amino acids 904−923, Figure 1, underlined) into the HK-M0 vector did not promote glycosylation of the translated product in the presence of microsomal membranes (Figure 7, lanes 1 and 2). In the HK-M1 vector, the H10 sequence did not prevent glycosylation of the β-region of the fusion protein (Figure 7, lanes 3 and 4), thus indicating that H10, similarly to H4, cannot act as an SA or an ST sequence.

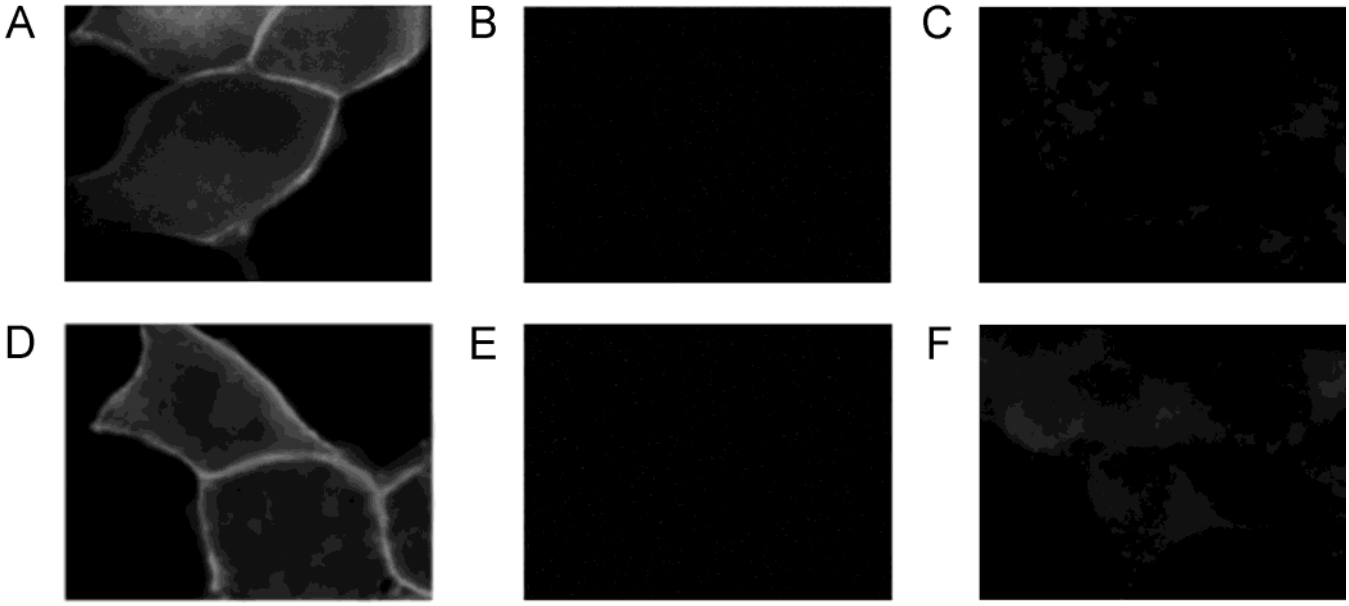

FIGURE 8: Immunolocalization of pNBC1 expressed in HEK293-T cells. In panels A, B, D, and E, the cells were transfected with a pcDNA3.1 plasmid containing the coding region of human pNBC1. In panels C and F, the cells were mock-transfected with the pcDNA3.1 plasmid only. (A) Cells permeabilized with methanol and stained with the N-terminal pNBC1 polyclonal antibody. (B) Nonpermeabilized cells stained with the N-terminal pNBC1 polyclonal antibody show no interaction of the antibody with the N-terminal epitope. (C) Mock-transfected cells permeabilized with methanol and stained with the N-terminal pNBC1 polyclonal antibody. (D) Cells permeabilized with methanol and stained with the C-terminal pNBC1 polyclonal antibody. (E) Nonpermeabilized cells stained with the C-terminal pNBC1 polyclonal antibody show no interaction of the antibody with the C-terminal epitope. (F) Mock-transfected cells permeabilized with methanol and stained with the C-terminal pNBC1 polyclonal antibody.

H11. The sequence encoding H11 (amino acids 950−967, Figure 1) exhibited both an SA and ST properties in the presence of microsomal membranes. The H11 sequence promoted glycosylation when inserted into the HK-M0 vector (Figure 7, lanes 5 and 6) and prevented glycosylation when inserted into the HK-M1 vector (Figure 7, lanes 7 and 8). According to the proposed pNBC1 model (Figure 2), H11 corresponds to putative TM9, which is predicted to have an SA activity.

H12. The HS12 (amino acids 971−986, Figure 1) inserted in the HK-M0 vector promoted glycosylation of the translated fusion protein in the presence of microsomes (Figure 7, lanes 9 and 10). Insertion of the same cDNA sequence into the HK-M1 vector prevented the translated protein form being glycosylated in the presence of microsomes (Figure 7, lanes 11 and 12). These data indicate that H12 corresponding to putative TM10 has both SA and ST properties.

Further Analysis of H10. According to the hydrophobic profile of pNBC1 (Table 2, Figure 1), the HS10 insert can potentially act as a transmembrane domain; however, insertion of this sequence into the HK-M0 and HK-M1 vectors demonstrated that HS10 has neither independent SA nor ST properties (Figure 7, lanes 1−4). To determine whether HS10 indeed lacks transmembrane activity in the context of the natural sequence of pNBC1, a construct containing HS10 between the flanking transmembrane domains (HS9 and HS11) was inserted into the HK-M0 and HK-M1 vectors.

HS9−HS11 Construct (amino acids 882−967). This construct would contain either a pair of transmembrane segments H9 and H11, as found with individual analysis, or three transmembrane segments if H10 is able to insert when it is in the context with the native pNBC1 sequence. Insertion of the construct HS9−HS11 into the HK-M0 vector resulted in only slight glycosylation of the translated product in the presence of microsomal membranes (Figure 7, lanes 13 and 14) as if this construct contained mainly a pair of membrane segments. This band disappeared upon deglycosylation (data not shown). When the HS9−HS11 construct was inserted into the HK-M1 vector, a glycosylated translation product was obtained in the presence of microsomal membranes (Figure 7, lanes 15 and 16), confirming that the tested sequence contains two but not three transmembrane domains. In fact, predicted orientations of the HS9 and HS11 inserts in the proposed pNBC1 model (Figure 2) and their orientations in the HK-M1 vector are the same.

Cytoplasmic Localization of the N-and C-Termini. The cytoplasmic localization of the pNBC1 N- and C-termini, was predicted on the basis of the distribution of positive charges and was confirmed using immunocytochemical studies in which antibodies raised against amino acids 1−19 in the N-terminus, and amino acids 1045−1050 in the C-terminus were utilized. As shown in Figure 8, both antibodies could bind their epitopes only after cell permeabilization, indicating that the N- and C-terminal epitopes are located intracellularly.

DISCUSSION

In this paper we present the membrane topography of human pNBC1, determined using an in vitro transcription/translation analysis in the presence of canine pancreatic microsomal membranes. To date, the structure of pNBC1 and other sodium bicarbonate cotransporters have been predicted based only on hydropathy algorithms. Hydropathy analyses of pNBC1 predict from 9 to 11 transmembrane domains (Table 2). In the present study, we show that pNBC1 contains 10 transmembrane domains with cytoplasmic localization of the N- and C-termini.

Cell-free in vitro transcription/translation analysis used in the current study of pNBC1 has proven to be predictive of the membrane topography of the CadA ATPase of *H. pylori* (*33*), the CCK-A receptor (*34*) and of the intestinal Na-bile acid cotransporter (*35*). It was also very useful in determining the membrane topography of other polytopic integral membrane proteins, such as the gastric H,K-ATPase (*31*), the ER−Ca-ATPase (*32*), and Na^+/H^+ exchanger NHE3 (*36*). Moreover, in later studies, the in vitro behavior of selected hydrophobic sequences of the H,K-ATPase were shown to act in an identical manner when expressed in oocytes and HEK 293 cells (*34*).

The in vitro transcription/translation method is based on the ability of polytopic integral membrane proteins to translocate into the membrane of the endoplasmic reticulum cotranslationally with sequentially alternating SA and ST sequences. The insertion of individual hydrophobic amino acid sequences or their combinations into the fusion proteins with well determined membrane topography and glycosylation sites (*31*) has allowed analysis of the insertion properties of the hydrophobic sequences of pNBC1 and thus the entire membrane topography of the protein. The in vitro transcription/translation analysis, however, may only partially reflects the intracellular environment and thus must be interpreted with caution when defining the actual membrane domain of a multi-segment integral membrane protein. Since most of the putative transmembrane domains of the pNBC1 exhibited both SA and ST properties, their proper orientation in the plasma membrane was deduced based on the location of the N- and C-termini. The cytoplasmic localization of the pNBC1 N- and C-termini was predicted on the basis of the distribution of positive charges, and was confirmed using immunocytochemical studies.

HEK293-T cells transfected with pNBC1 expressed the transporter predominantly on the plasma membrane as we have previously shown (*21*). Permeabilization of the cells was required to detect any immunoreactivity with antibodies directed against the N and C-termini. These data indicate that both the N- and C-termini of pNBC1 are located intracellularly, which predicted an even number of transmembrane domains. This is further supported by the fact that the in vitro transcription/translation analysis identified 10 transmembrane domains. Taken together, the results of our study define the actual membrane orientation of the hydrophobic transmembrane sequences, which is reflected in the proposed pNBC1 model in Figure 2. The first N-terminal transmembrane domain and subsequent odd-numbered domains function as SA sequences, whereas the even-numbered domains function as ST sequences.

The experimental data presented above show that the tested hydrophobic sequences H1, H2N, H3CE, H5, H7, H9CE, H11, and H12 possess both an SA and ST properties, whereas sequences H6 and H8CE show only SA activity. The extension of H3 and H9 sequences in the C-terminal direction provides each of these with ST activity. Although, based on the hydropathy profiles of pNBC1, the C-terminal extensions of H3CE and H9CE are perhaps parts of the extracytoplasmic and cytoplasmic loops, respectively, they seems to be necessary for exhibiting effective membrane insertion properties in the in vitro translation system, regardless of their orientation in the predicted pNBC1 topography model. It has been suggested that positively charged amino acids present in upstream or downstream sequences flanking a putative transmembrane domain (*34*, *40*−*45*), as well as cooperative action of adjacent transmembrane domains (*36*, *46*), have the ability to increase insertion efficiency of hydrophobic sequences. Our results with C-terminal extensions further suggest that membrane insertion and orientation of putative hydrophobic domains is a process that can be controlled by as few as three uncharged amino acids following immediately after defined hydrophobic regions. Similar to H3 and H9 hydrophobic domains, the C-terminal extension of H8 increases insertion efficiency of this sequence. Although in this case the elongated sequence shows only strong SA activity, the C-terminal extension of the HS8 insert is still necessary for the effective anchoring of this transmembrane domain into the plasma membrane. On the basis of the hydrophobicity profile of the region around the H8 sequence, this C-terminal extension is most likely a part of the extracellular loop. The lack of ST activity shown by H8CE fragment is probably due to the fact that in the predicted pNBC1 topography model, this hydrophobic sequence has an SA orientation. It is possible that the hydrophobic sequence H6 lacks ST activity for the same reason that, according to our pNBC1 topography model, it is predicted to have a SA orientation in the plasma membrane. In fact, the finding that H8CE and H6 act in only one orientation is compatible with the predicted topographic model of pNBC1. These data suggest that H6 and H8CE do not partner effectively with the M1 of the H,K-ATPase, in contrast to the other membrane sequences of pNBC1.

Hydrophobic sequences H4 and H10, inserted alone into the HK-M0 and HK-M1 vectors, showed neither SA nor ST properties, suggesting that these sequences lack transmembrane activity. The variants of H4 (H4CE, H4CS) still lacked either SA or ST activities. The N-terminal extension of H4 to include the preceding putative hydrophobic sequence H3 still did not provide H4 with ST activity, which would have been the expected orientation for this sequence if it were a part of the membrane domain of pNBC1. Furthermore, when H4 was extended in the N-terminal direction up to the beginning of H2N, the same absence of ST activity on the part of H4 was observed, providing evidence that H4 is a part of an extracellular loop, rather than a transmembrane domain. In fact, only four predictive hydrophobicity algorithms out of eight suggested that this region of pNBC1 contains a putative hydrophobic sequence (Table 2), and two (Kyte−Doolittle (*47*) and TMpred (*48*)) out of these four algorithms gave the lowest hydrophobicity score to the HS4 sequence. Moreover, an alternative model of pNBC1 offered by TMpred algorithm (*48*) does not even consider H4 sequence as a putative hydrophobic sequence. Similarly to H4, only four computer algorithms (Table 2) predicted the H10 sequence as a membrane domain. Insertion of H10 along with the adjacent sequences (H9 and H11) into the HK-M0 and HK-M1 vectors provided evidence that H10 does not have transmembrane activity, and is a part of the intracellular loop that links TM8 and TM9. In addition, the glycosylation observed in the HK-M0 vector with H9−H11 construct suggests that the membrane inserted sequences H9 and H11 integrate into the plasma membrane according to their native orientations (Figure 2).

Examination of the putative transmembrane domains in the proposed pNBC1 model reveals that TM8 contains a

positively charged lysine residue, while TM3 contains one and TM5 has two aspartate residues. The importance of charged residues within transmembrane hydrophobic sequences has been previously documented in many membrane transporters (*49*−*51*). One possible role is the pairing of oppositely charged residues to form charge pairs, within and between transmembrane domains, which could be essential for their packing and maintenance of the native structure of the protein (*49*−*51*). Another possible role of charged residues is in ion binding. Previous studies of membrane transporters suggested that negative residues participate in cation binding (*52*), while positive residues may participate in anion binding (*53*, *54*). In addition to the charged residues within TM3, TM5, and TM8, all 10 of the proposed transmembrane sequences have a charged or hydrophilic residue at their ends which could be the actual boundary of each. Definitive determination of the pNBC1 transmembrane topography awaits a crystal structure of the cotransporter.

REFERENCES

1. Gross, E., Abuladze, N., Pushkin A., Kurtz I., and Cotton, C. U. (2001) *J. Physiol. 531*, 375−82.
2. Marino, C. R., Jeanes, V., Boron, W. F., and Schmitt, B. M. (1999) *Am. J. Physiol. 277*, G487−94.
3. Abuladze, N., Lee, I., Newman, D., Hwang, J., Boorer, K., and Pushkin, A., Kurtz, I. (1998) *J. Biol. Chem. 273*, 17689−95.
4. Casey, J. R., and Reithmeier, R. (1998) *Biochem. Cell Biol. 76*, 709−13.
5. Alper, S. L. (1991) *Annu. Rev. Physiol. 53*, 549−64.
6. Wang, C. Z., Yano, H., Nagashima, K., and Seino, S. (2000) *J. Biol. Chem. 275*, 35486-90.
7. Romero, M. F., Henry, D., Nelson, S., Harte, P. J., Dillon, A. K., and Sciortino, C. M. (2000) *J. Biol. Chem. 275*, 24552−9.
8. Grichtchenko, I. I., Choi, I., Zhong, X., Bray-Ward, P., Russell, J. M., and Boron, W. F. (2001) *J. Biol. Chem. 276*, 8358−63.
9. Pushkin, A., Abuladze, N., Lee, I., Newman, D., Hwang, J., and Kurtz, I. (1999) *Genomics 58*, 321−2.
10. Pushkin, A., Abuladze, N., Lee, I., Newman, D., Hwang, J., and Kurtz, I. (1999) *J. Biol. Chem. 274*, 16569−75.
11. Ishibashi, K., Sasaki, S., and Marumo, F. (1998) *Biochem. Biophys. Res. Commun. 246*, 535−8.
12. Choi, I., Aalkjaer, C., Boulpaep, E. L., and Boron, W. F. (2000) *Nature 405*, 571−5.
13. Sassani, P., Pushkin, A., Gross, E., Gomer, A., Abuladze, N., Dukkipati, R., Carpenito, G., and Kurtz, I. (2002) *Am. J. Physiol. 282*, C408−16.
14. Pushkin, A., Abuladze, N., Newman, D., Lee, I., Xu, G., and Kurtz, I. (2000) *Biochim. Biophys. Acta 1493*, 215−8.
15. Pushkin, A, Abuladze, N., Newman, D., Lee, I., Xu, G., and Kurtz, I. (2000) *IUBMB Life 50*, 13−9.
16. Abuladze, N., Song, M., Pushkin, A., Newman, D., Lee, I., Nicholas, S., and Kurtz, I. (2000) *Gene 251*, 109−22.
17. Abuladze, N., Lee, I., Newman, D., Hwang, J., Pushkin, A., and Kurtz, I. (1998) *Am. J. Physiol. 274*, F628−33.
18. Schmitt, B. M., Biemesderfer, D., Romero, M. F., Boulpaep, E. L., and Boron, W. F. (1999) *Am. J. Physiol. 276*, F27−38.
19. Burnham, C. E., Amlal, H., Wang, Z., Shull, G. E., and Soleimani, M. (1997) *J. Biol. Chem. 272*, 19111−4.
20. Ross, E., and Kurtz, I. (2002) *Am. J. Physiol. 281*, F876−87.
21. Bok, D., Song, M., Pushkin, A., Sassani, P., Abuladze, N., Naser, Z., and Kurtz, I. (2001) *Am. J. Physiol. 281*, F920−35.
22. Romero, M. F., Hediger, M. A., Boulpaep, E. L., and Boron, W. F. (1997) *Nature 387*, 409−13.
23. Tang, X. B., Fujinaga, J., Kopito, R., and Casey, J. R. (1998) *J. Biol. Chem. 273*, 22545−53.
24. Jennings, M. L., and Smith, J. (1992) *J. Biol. Chem. 267*, 13964−71.
25. Jennings, M. L., and Anderson, M. P. (1987) *J. Biol. Chem. 262*, 1691−7.
26. Muller-Berger, S., Karbach, D., Konig, J., Lepke, S., Wood, P. G., Appelhans, H., and Passow, H. (1995) *Biochemistry 34*, 9315−24.
27. Tang, X. B., Kovacs, M., Sterling, D., and Casey, J. R. (1999) *J. Biol. Chem. 274*, 3557−64.
28. Fujinaga, J., Tang, X., and Casey, J. R. (1999) *J. Biol. Chem. 274*, 6626−33.
29. Taylor, A. M., Zhu, Q., and Casey, J. R. (2001) *Biochem. J. 359*, 661−8.
30. Popov, M., Tam, L., Li, J., and Reithmeier, R. A. (1997) *J. Biol. Chem. 272*, 18325−32.
31. Bamberg, K., and Sachs, G. (1994) *J. Biol. Chem. 269*, 16909−19.
32. Bayle, D., Weeks, D., and Sachs, G. (1995) *J. Biol. Chem. 270*, 25678−84.
33. Melchers, K., Weitzenegger, T., Buhmann, A., Steinhilber, W., Sachs, G., and Schafer, K. P. (1996) *J. Biol. Chem. 271*, 446−57.
34. Bayle, D., Weeks D., and Sachs, G. (1997) *J. Biol. Chem. 272*, 19697−707.
35. Hallen, S., Branden, M., Dawson, P. A, and Sachs, G. (1999) *Biochemistry 38*, 11379−88.
36. Zizak, M., Cavet, M., Bayle, D., Tse, C. M., Hallen, S., and Sachs, G., Donowitz, M. (2000) *Biochemistry 39*, 8102−12.
37. Reuben, M. A., Lasater, L., Sachs, G. (1990) *Proc. Natl. Acad. Sci. U.S.A. 87*, 6767−71.
38. Sambrook, J., Fritsch, E. F. and Maniatis, T. (1989) *Molecular Cloning: A Laboratory Manual*, 2 ed., Cold Spring Harbor Laboratory Press, Cold Spring Harbor, NY.
39. Sardet, C., Counillon, L., Franchi, A., and Pouyssegur, J. (1989) *Science 247*, 723−6.
40. von Heijne, G., and Gavel, Y. (1988) *Eur. J. Biochem. 174*, 671−8.
41. von Heijne, G. (1989) *Nature 341*, 456−8.
42. Nilsson, I., and von Heijne, G. (1990) *Cell 62*, 1135−41.
43. Beltzer, J. P., Fiedler, K., Fuhrer, C., Geffen, I., Handschin, C., Wessels, H. P., and Spiess, M. (1991) *J. Biol. Chem. 266*, 973−8.
44. von Heijne, G. (1992) *J. Mol. Biol. 225*, 487−94.
45. Andersson, H., and von Heijne, G. (1994) *FEBS Lett. 347*, 169−72.
46. van Geest, M., Nilsson, I., von Heijne, G., and Lolkema, J. S. (1999) *J. Biol. Chem. 274*, 2816−23.
47. Kyte, J., and Doolittle, R. (1982) *J. Mol. Biol. 157*, 105−32.
48. Stoffel, W., and Hofmann, K. (1993) *Biol. Chem. Hoppe-Seyler 374*.
49. Sahin-Toth, M., and Kabak, H. (1993) *Biochemistry 32*, 10027−35.
50. Lee, J. I., Hwang P., and Wilson, T. H. (1993) *J. Biol. Chem. 268*, 20007−15.
51. Dunten, R. L, Sahin-Toth, M., and Kaback, H. R. (1993) *Biochemistry 32*, 3139−45.
52. Yerushalmi, H., and Schuldiner, S. (2000) *Biochemistry 39*, 14711−9.
53. Fu, D., Sarker, R., Abe, K., Bolton, E., and Maloney, P. C. (2001) *J. Biol. Chem. 276*, 8753−60.
54. Kolbe, M., Besir, H., Essen, L. O., and Oesterhelt, D. (2000) *Science 288*, 1390−6.
55. Claros, M. G., and von Heijne, G. (1994) *Comput. Appl. Biosci. 10*, 685−6.
56. Persson, B., and Argos, P. (1996) *Protein Sci. 5*, 363−371.
57. Jones, D. T., Taylor, W., and Thornton, J. M. (1994) *Biochemistry 33*, 3038−49.
58. http://sosui.proteome.bio.tuat.ac.jp/sosuiframe0.html.
59. Moller, S. M., Croning, D. R., and Apweiler, R. (2001) *Bioinformatics 17*, 646−53.
60. Tusnady, G. E., and Simon, I. (1998) *J. Mol. Biol. 283*, 489−506.

BI026826Q